ASSESSMENT OF THE RESIDUAL EXPANSION FOR EXPERTISE OF STRUCTURES AFFECTED BY AAR

A. Sellier[1*], E. Bourdarot[2], S. Multon[1], M. Cyr[1], E. Grimal[2]

[1]Université de Toulouse ; UPS, INSA ; LMDC (Laboratoire Matériaux et Durabilité des Constructions), 135, avenue de Rangueil ; F-31077 TOULOUSE Cedex 04, France

[2] Electricité de France : Centre d'Ingénierie Hydraulique, EDF- CIH Technolac F-73373 LE BOURGET DU LAC Cedex, France

Abstract

Alkali aggregate reaction (AAR) causes premature and unrecoverable deteriorations of numerous civil engineering structures. AAR-expansions and induced cracking can affect the functional capacity of bridges and dams. Several hydraulic dams of Electricité de France (EDF) are concerned by AAR. Therefore, a behaviour model implemented in a finite element code has been developed in order to assess the safety level and the maintenance choices of these degraded structures. This approach has the particularity of modelling the AAR structural effects from the construction of the structure until today. It uses several AAR advancement variables, one for each aggregate size range of the affected concrete. These advancement variables depend on both the saturation degree and the temperature in the dam. At first, this paper presents an historical review of the Temple sur Lot dam. On this dam, built between 1948 and 1951, first cracks were observed in 1964. Several remedial work campaigns have been carried out since 1970. Recent deformation measurements showed that expansions keep on. In a second part, the difficulty of using a classical residual expansion test on core samples to fit the model is pointed out, particularly when the swelling rate is slow due to low alkali content in the concrete. Thus, the authors propose an original approach combining additional tests and physical modelling to assess the chemical advancement of the AAR for each aggregate size of the affected concrete. Only the chemical advancement, which is a normalized variable linked to the residual reactive silica content, is measured in laboratory. The concrete residual potential expansion is not measured on laboratory tests but fitted through an inverse analysis based on a finite element structural calculation. This calculation takes into account the geometry, the thermo-hydro-mechanical environment of the structure and the measured displacement rates. This combination of chemical analysis in laboratory and structural displacement measurements allows a reliable model fitting. In fact, damages and displacements calculated on several points (not used for the model fitting) of the Temple-sur-Lot dam can be found with an acceptable accuracy. Thus a prediction of the dam behaviour can be made for the next decades.

Keywords: Alkali aggregate reaction, expansion, structural expertise, dams, finite element

1 INTRODUCTION

The dam of Temple sur Lot was built in 1948 but since 1964, abnormal expansion resulting in significant and continuous structure displacements is monitored. Extensive analyses of concrete cores confirmed that these movements could be attributed to AAR, despite low and relatively constant alkali content in the concrete one the one hand, and non-significant residual swelling test results on the other hand.

The authors showed, by using SEM analysis on AAR gel, that a substitution process of alkalis by calcium could explain the long term behaviour of the dam. Since the calcium substitution is very slow, it cannot be detected using a classical residual swelling test, so an original method is proposed to assess the potential AAR-expansion remaining in the dam and the kinetic of AAR development.

This method is divided in two steps. The first one involves laboratory tests dealing with the chemical kinetic of AAR. The second step is a numerical simulation of the dam using finite element calculations. It allows the fitting of final swelling amplitude on observed displacement rates.

The capability of the model to predict expansions and movements of the dam is validated through a comparison between calculations and measurements of monitored spots which are not used

* Correspondence to: alain.sellier@insa-toulouse.fr

for the model development. Then, a predictive evaluation of the dam's behaviour (displacements and damages) is calculated for the next decades.

2 TEMPLE SUR LOT DAM PRESENTATION

The dam of Temple sur Lot, located in the south-west of France has been operating since 1951. It includes a gate-structure dam equipped with four double leaf vertical lift gates (20 m wide, 10 m high) and a power-house with two Kaplan turbines (Figures 1 (a) and (b)). As soon as 1963, an inspection revealed the existence of cracks on the upstream part of dam piers. In the following years, difficulties in the operation of the bulkhead gates induced several interventions on the mechanical parts embedded in the concrete structure. Reinforcement of the monitoring system provided a better description of deformation of the piers and laboratory investigations pointed out the existence of swelling phases inside the concrete. During the period 1983-1988, extensive works were carried out on the piles: anchoring, epoxy and polyurethane grouting. Recently (2002-2003), the guidance system of the gates has been modified in order to absorb concrete deformations. Indeed the effects of the swelling process on the structure are of several orders: general rising of the piers (1mm / year) and tilting of the lateral piers toward the gates (0.6, 0.9 mm/year). If the symmetrical movements of the central piers seem comprehensible, the horizontal movements of the lateral piers, explaining the difficulties observed in the operation of the corresponding gates, appear more difficult to justify. Several reasons were given, in particular the existence of steel reinforcements on the external faces of the piers, the dissymmetry of the humidity conditions or structural effects. In order to explain these particularities, to make an overall evaluation of the stability of the dam, and to plan its long term management, an investigation and study program has been decided including a reinforcement of the monitoring system (installation of a pendulum line and a long base extensometer in the drainage gallery), laboratory investigations and finite element modelling. In this respect, one of the main questions to address is the estimation of the residual expansion of concrete.

3 CORE SAMPLES RESIDUAL EXPANSION TESTS LIMITS

Initially, classical residual expansion tests [1] [2] [4] were carried out at LMDC for EDF according to the LPC method [14]. This method consists in measuring the longitudinal expansion and the mass variation of core samples (14 cm diameter, 30 cm length) drilled from the dam and kept into a controlled environment (38°C, relative humidity > 95%). For each concrete type of the dam (C350 and C250 in Figure 2), three core samples were instrumented by three vertical plots lines between which a longitudinal measure was periodically done. Mean values and scattering of these measurements are shown in Figure 3. After eight weeks, the mass was stabilized. During this first period, the strain variations are explained by the shrinkage comeback due to the water imbibitions (Figure 3). So, even if a part of this first expansion is due to AAR [17], this part of the curve is difficult to use. After this period, the LPC's method attributed the strain variations to AAR. The swelling trend is represented in Figure 3 by the dotted lines. The swelling rate was about 100 μm/m/year. According to the LPC's recommendations, this value corresponded to a negligible AAR phenomenon, which was in disagreement with the in-situ observations on the dam. The interpretations of the swelling rates by the LPC recommendations seemed not suitable for this dam. Moreover, the tests did not give information about the residual swelling capability of the concrete since the final swelling was not reached after one year (no asymptotic aspect of the curve in Figure 3). Therefore, the authors decided to develop a different experimental process to assess both the kinetic and the residual swelling capability of the AAR affected concrete.

4 PROPOSED EXPERIMENTAL PROCESS

Based on previous works on the size effect of reactive aggregates on the swelling capability of mortars [19] [16], the authors propose a new procedure to assess residual swelling capability of concrete. This process consists in splitting the problem in three different phases:

1- After a recovery of the aggregates by selective dissolution of the cement paste, the chemical advancement is assessed for each reactive aggregate size using a specific accelerated procedure.

2- The in-situ chemical advancement kinetic is deduced from the advancement measured for each aggregate size.

3- The concrete final swelling amplitude is fitted to reproduce observed in situ displacement rate using a finite element modeling [5] [6]. This step combines advancement kinetic measured in laboratory and fitted final AAR swelling. Once the final swelling has been fitted, numerical modeling is tested on dam's zones which were not used for the fitting. If the results areaccurate , calculations can be carried out to predict the future structural behavior of the dam.

Hence, the method originality consists in splitting the calibration procedure of the model in a chemical way studied in laboratory, and in a mechanical way based on a numerical modelling of the affected structure. The chemical study deals with the chemical advancement determination independently of the final swelling, and the numerical simulation allows fitting the final swelling amplitude compatible with both the chemical advancement measured in the laboratory and the in-situ observed swelling rate. This approach allows an original combination of in situ displacement measurements exploitation and laboratory chemical analysis. Its main advantage is to treat properly the environmental effects on AAR through the finite element modelling boundaries conditions.

4.1 First phase: Chemical advancement determination

Principle

According to Poyet [19], the authors assume that, if the alkali content is sufficient, a reactive aggregate having a volume V_a can create a maximal gel volume V_g (Eq 1) proportional to its own volume:

$$V_g = f \cdot V_a \tag{1}$$

Practically several aggregate sizes can be successively studied; their volume V_a can be approximated assuming spherical aggregates having an average diameter defined by the one passing between two consecutive sieves. The proportionality factor *f* depends on the reactive silica content of the aggregate and on the gel texture. It is different for alkali-silica gel and calcium-silica gel. As explained by Poyet and al. [19], the gel volume can lead to a swelling phenomena only if the connected porosity to the reactive aggregate (V_p in Eq 2) has been entirely filled by the gel, the free swelling can then be approximated by a linear relation (Eq 2), in which *n* is the volumetric number of reactive aggregate with a given size in the concrete . $\langle\ \rangle$ means "positive part".

$$\varepsilon = n \cdot \langle V_g - V_p \rangle \tag{2}$$

According to Poyet and al, the connected porosity is assumed to be proportional to the aggregate surface, it can be idealized by a *lc* thickness porous rim (Eq 3) surrounded the spherical idealized aggregate.

$$V_p = \frac{4}{3}\pi \left[\left(R_a + l_c\right)^3 - R_a^{\ 3} \right] p \tag{3}$$

where R_a is he aggregate radius and *p* is the surrounding material porosity. When the reactive silica of the aggregate is totally consumed by the AAR, its final free volumetric swelling contribution is approximated by Eq (4).

$$\varepsilon^{\infty} = n \left\langle f\ V_a - V_p \right\rangle \tag{4}$$

If the aggregate under consideration has already partially reacted into the structure (before the test, i.e between t=0 (the building date) and t=T (the test date)), its residual swelling potential ε^{res} (Eq. 5) depends on the chemical advancement A_T of the AAR at the extraction moment T (equal to the test date), as indicated in Eq 5.

$$\varepsilon^{res} = n \left\langle f\, V_a \left(1 - A_T\right) - V_p \right\rangle \tag{5}$$

The objective of the laboratory experimental procedure is to assess the advancement A_T for each aggregate size range of each concrete of the structure.

Application to the dam's concrete

Chemical attacks and sieving have been carried out for the two concrete types of the Temple sur Lot dam as mentioned in Figure 4. In order to measure the residual swelling potential, three prismatic mortar specimen (2x2x16 cm) have been cast for each concrete aggregate size range (each mortar in Figure 4). The splitting in two mortar types for each concrete aggregate size distribution (presented in Figure 4) is chosen to limit the number of mortars, but a splitting in more size ranges could lead to a better accuracy. Each mortar contains only a single aggregate size range of each concrete. The corresponding concrete aggregates have been crushed and sieved to retain only the size ranging from 0.16 to 3.15 mm as mentioned in Figure 4. According to previous works [19] [8] [15] [16], smaller particles lead to lower swelling and larger particles lead to important but slower swelling. The total amount of crushed reactive aggregates, their size (after crushing) and the alkali content must be the same for all the mortars. An alkali content of about 8 kg/m^3 is chosen to get a total consumption of the residual reactive silica (over this value, the final swelling becomes independent of the alkali content for this aggregate). This choice is required to verify the assumption associated to Eq 1 (total consumption of residual reactive silica). Hence mortar differs from each other only by their residual reactive silica content proportion included in the aggregates. Therefore if a mortar presents a greater swelling than another one, it means that its residual reactive silica content is higher. In other words, and according to Eq 5, its associated "in-situ" chemical advancement A_T is smaller.

After a 28 days of curing in sealed bags at 20°C, specimens have been put into a reactor at 95% HR and 60°C. The longitudinal strain and the mass variations have been periodically measured, due to the geometry of the specimens (small transversal dimension cf. [20]), the mass variations were stabilized a few days after the specimens have been put into the reactor and their fluctuations were negligible during the test. The expansions measured on the specimens have been plotted in Figure 5.

It shows that the concrete gravels have a bigger residual swelling capability than the sands. In fact, due to the diffusion mechanism [3], alkali and hydroxyl ions ingress in larger concrete aggregates concerns only the periphery as shown in Figure 6. A large zone of unaltered silica stays in the core of the aggregate. When such aggregates are crushed before making the mortar, most of the crushed aggregates have a low AAR average advancement. Consequently, they lead to a large residual swelling (G250 in Figure 5). At the opposite, the alkali and hydroxyl ions ingress concerns a larger relative zone in the concrete sand where more reactive silica is reached by the ions. It leads to a larger advancement in the concrete and a smaller residual swelling for the corresponding laboratory's mortars (for example S350 in Figure 5). Finally, residual swelling on mortar made with crushed aggregates show that larger aggregates contain more unaltered silica and lead to greater residual swelling than smaller ones. Moreover, Figure 5 points out that swelling capability decreases with the concrete cement content. The amounts of alkali and hydroxyl ions in the dam's concretes are proportional to the cement contents. Therefore, the aggregate contained in the concrete with a cement content of 350 kg/m^3 are more altered than the aggregate of the concrete with a cement content of 250 kg/m^3. Consequently they lead to smaller residual swelling.

Therefore, it can be concluded that the chemical advancement of the AAR, in each concrete aggregate, depends on the concrete cement content and on the aggregate size. According to Eq 5, the silica consumption can be divided in two parts: a first phase occurs in the structure and a second phase is provoked in the laboratory tests on mortars (Figure 7). The swelling curves are then used only in order to assess the advancement of the reaction A_T before the beginning of the accelerated test. Theoretical swellings of each mortar can be calculated using Eq 5. In this equation, all parameters are the same for the four mortars, excepted the value of the initial chemical advancement A_T which depends, as explained above, on the aggregate size and on the cement content in the concrete. In order to assess these advancements a least square method can be used: A global error E (Eq 6) corresponding to the cumulated square deviations between the final swellings measured on specimens $\varepsilon_{\exp}^{res(mortar)}$ and the theoretical values computed with Eq. 5 $\varepsilon_{th}^{res(mortar)}$ is built (Eq 6). The minimization of this error leads to A_T and f values given in Table 1.

$$E = \sum_{mortar}\left(\underbrace{n\left\langle f\,V_a\left(1 - A_T^{mortar}\right) - V_p\right\rangle}_{\varepsilon_{th}^{res(mortar)}} - \varepsilon_{\exp}^{res(mortar)}\right)^2 \qquad (6)$$

As required and explained above, the aggregate number n in each mortar is the same for the four formulations; it is taken equal to the mortar sand content (1500 kg/m^3) divided by the sand density and by the aggregate elementary volume (V_a). For V_p, a characteristic length lc (Eq 3) of 10 µm is adopted according to Poyet and al. work [19]. Even if a value is obtained for the parameter f by the fitting procedure, it cannot be used for the structural analysis. In fact, it corresponds to an alkaline gel induced by the high mortar alkali content, and not to the gel containing calcium as observed in the dam. Another value of f will be fitted on measured displacements on the dam via a finite element inverses analysis. This will be the last model calibration step.

4.2 Second phase: "in-situ kinetic" determination

In the finite element analysis a kinetic differential law proposed by Grimal et al. [5] [7] is used to model the "in situ kinetic" of the reaction:

$$\frac{\partial A}{\partial t} = \underbrace{\alpha_{20}\ .\exp\left(-\frac{E_a}{R}\left(\frac{1}{273+\theta}-\frac{2}{293}\right)\right)}_{\alpha_0(\theta)}\frac{\langle Sr - Sr^0\rangle}{(1-Sr^0)}\langle Sr - A\ \rangle \tag{7}$$

where α_{20} is the kinetic constant to be fitted, Sr the saturation degree and Sr^0 the saturation degree threshold upper which the reaction occurs (estimated to 40%, according to the Poyet's experimental results [20]), θ (in °C) the temperature in the dam's zone where the concrete has been drilled, E_a the activation energy of the reaction. A temperature-dependent kinetic parameter $\alpha_0(\theta)$ can also be defined from Eq. 7. This parameter is calculated from the mortar tests. Afterward α_{20} can be deduced from $\alpha_0(\theta)$ and used in the dam finite element analysis. The relation between the advancement A_T determined with mortar tests (A_T=A_T^{mortar} from Eq 6) and the kinetic parameter is the result of the differential form (Eq. 7) integration from the building date ($\tau = 0$) to the test date ($\tau = T$). This integration (Eq. 8) takes into account the real environmental conditions: humidity through $\overline{S}_r$ (the time-averaged saturation degree) and $\overline{\theta}$ (the time-averaged temperature) of the in-situ concrete in the dam's zone where the core samples have been drilled.

$$A_T = \int_{\tau=0}^{\tau=T}\frac{\partial A(Sr(\tau),\theta(\tau))}{\partial t}d\tau \approx \int_{\tau=0}^{\tau=T}\frac{\partial A(\overline{S}r,\overline{\theta})}{\partial t}d\tau = \left[1-\exp\left(-\alpha_0(\overline{\theta})\frac{\overline{S}r\ \ - Sr^0}{1-Sr^0}T\right)\right] \tag{8}$$

As said above, the in situ saturation degree ($\overline{S}_r$) must be measured on specimens taken from the dam (by dry sawing to avoid humidity perturbation). T is the dam's age (60 years for Temple sur Lot).
A characteristic time τ of the reaction advancement for each concrete aggregate type can also be defined from (Eq. 8) and linked to the "in-situ kinetic constant":

$$\begin{aligned}\tau &= -\frac{T}{\ln\left(1-A_T\right)}\\ \alpha_0 &= \frac{1}{\tau\,\dfrac{Sr\ \ - Sr^0}{1-Sr^0}}\end{aligned} \tag{9}$$

The characteristic time of the kinetic advancement is not explicitly used in the modelling but corresponds to the required time to reach an advancement A of 63%. It is about 60 years for the C350 sand and about 522 years for the C250 large gravel (Table 1). These results are in accordance with the observations made on the specimens (Figure 5). Indeed, the reaction appears to be almost finished for the sand of the concrete with 350 kg/m³ of cement but not so advanced for the second concrete largest gravels. Thus, if the alkalinity of the cement matrix is kept up into the dam, the AAR will go on. It can be noted that a substitution reaction between alkali of the initial AAR gel and calcium of the cement paste [9] can maintain the alkalinity condition.

4.3 Third phase: "Final in-situ swelling amplitude" determination

As explained above, the fitting achievement consists in the determination of the constant *f* (Eq 2). The constant *f* obtained from the accelerated tests cannot be used for the dam's analysis because of the difference of ASR gel nature between the long term reaction in the dam (calcium-silica gel) and the short term reaction in the accelerated test (alkali-silica gel). In order to assess this constant, the model is fitted on the observed behaviour of the dam. The constant is then assessed by iteration to adjust the finite element model response (in terms of structural displacements) to the observations. In the calculations, the final swelling of concrete containing several aggregate size ranges is assumed to be the sum of the final swelling contributions of each aggregate size range (Eq 4 applied to the concrete).

In the dam, the swelling cannot be directly linked to the advancement (like in Eq 4): in fact, the structural effects lead to free swelling, which can decrease or increase according to the mechanical boundary conditions [10][12][18][21][24]. This is why the mechanical model is based, as in [23], on a poro-mechanical formulation [5] [6] (Eq. 10). In Eq. 10, the total strain ε is induced by both the gel pressure P_g acting into the concrete porosity and the mechanical stress σ induced by the structural loading and the capillarity pressure P_w. The anelastic strain ε^{an} includes a creep strain and an irreversible strain associated to the cracks opening [5].

$$\sigma = C(\varepsilon - \varepsilon^{an}) - b_g P_g - b_w P_w \tag{10}$$

In this equation *C* is the damaged stiffness tensor [22], b_g a parameter given the gel pressure influence on the concrete matrix [23]. The gel pressure (P_g) is linked to the AAR advancement A with the following equation taken from [5]:

$$P_g = M_g \sum_s \left\langle n^s A^s f V_a^s - \left\langle V_p^s + b_g tr(\varepsilon) \right\rangle \right\rangle \tag{11}$$

Superscript "*s*" is relative to a single concrete aggregate size range. The coefficient M_g in Eq 10 is the bulk coefficient of the gel. b_g and M_g fitting is explained in Grimal et al [6]. The chemical advancement A^s, for a given aggregate size, is computed using a numerical step by step integration of (12).

$$\frac{\partial A^s}{\partial t} = \alpha_{20}{}^s.\exp\left(-\frac{E_a}{R}\left(\frac{1}{273+\theta} - \frac{2}{293}\right)\right)\frac{\left\langle Sr - Sr^0 \right\rangle}{(1 - Sr^0)}\left\langle Sr - A^s \right\rangle \tag{12}$$

In Eq. 12, α_{20}^s ($s = \{S, G\}$) are the kinetics constants calculated according to the mortar free expansion (Table 1) and transposed to the dam's condition according to the definition of α_0 given in Eq 7.

Practically, only the variation of the lateral displacement measured on the point PC (Figure 8 and Figure 9 (a) direction yy) has been used to assess *f*. Then, the vertical displacements of PC (Figure 9 (a) direction zz) and the horizontal displacement of PA (Figure 9 (b)) can be simulated with a good accuracy. A prediction of the pier movements can thus be done for the next decades (Figure 9 (a) and (b)). The finite element structural modelling proposed in [5] [6] is also able to compute the damage into the dam due to the AAR evolution, as illustrated in Figure 10. The damage variable changes from zero for an undamaged material to one for a macroscopic crack. The damaged zones shown in Figure 10 are in good agreement with the crack pattern observed on the dam.

5 CONCLUSION

This paper presented a new method to predict the structural behaviour of a dam affected by AAR. The method, which was developed because of the difficulty of using classical accelerated residual swelling test, is based on two complementary fitting processes:

1- An experimental analysis of the affected concrete carried out in the laboratory, in order to assess the chemical kinetic of the reaction for each aggregate size of the concrete. The method used to compute the kinetic parameters includes environmental conditions such as the degree of saturation and the temperature of concrete in the dam.

2- A non linear finite element analysis of the structure carried out to fit the final swelling amplitude of the concrete. This step takes into account the displacement rates measured on the structure and the possible spatial and temporal variations of the environmental conditions.

The method was successfully tested on the dam of Temple sur Lot. The fitting of the amplitude using only one displacement of the dam combined with the laboratory determination of the chemical kinetic parameters allows other displacements of the dam and realistic damage to be calculated. Based on this work, a prediction of the dam's displacements and damage has been carried out for the next decades.

6 REFERENCES

[1] Bérubé, M.A., Smaoui, N., Côté, T., (2004) Expansion tests on cores from ASR-affected structures, Proc. 12th Int. Conf. AAR, Beijing, China, 821-832.

[2] Fasseu, P. and Mahut, B., eds (2003) Guide méthodologique : Aide à la gestion des ouvrages atteints de réactions de gonflement interne, LCPC, « techniques et méthodes des LPC » collection, Paris, France (in French).

[3] Furosawa Y., Ohga H., Uomoto T., 1994, "An analytical study concerning prediction of concrete expansion due to Alkali-Silica Reaction", 3rd CANMET/ACI International Conference on Durability of Concrete, Nice, France, pp. 757-779.

[4] Godart, B., Fasseu, P. and Michel, M., (1992) Diagnosis and monitoring of concrete bridges damaged by AAR in Northern France, Proc., 9th Int. Conf. AAR, London, England, 368-375.

[5] Grimal E, Sellier A., Le Pape Y., Bourdarot E., "Creep shrinckage and anisotropic damage in AAR swelling mechanism, part I: a constitutive model", accepted on 25-Jan-2008 for publication in the American Concrete Institute Material Journal.
[6] Grimal E, Sellier A., Le Pape Y., Bourdarot E., "Creep shrinckage and anisotropic damage in AAR swelling mechanism, part II : a FEM anlysis" , accepted on 13-Feb-2008 for publication in the American Concrete Institute Material Journal.
[7] Grimal E., Sellier A., Le Pape Y., Bourdarot E., « Influence of moisture and cracking on aar degradation process : impact on concrete structural behaviour using fem anlysis", Int Conference on Concrete under Severe conditions : Environment & Loading, F.Toulemonde edt, ISSN 1628-4704, pp. 757-765, Consec 07, Tour France, 4-6 juin 2007.
[8] Guédon-Dubied J.S., Cadoret G., Durieux V., Martineau F., Fasseu P., van Overbecke V., Study on Tournai limestone in Antoing Cimescaut Quarry. Petrological, chemical and alkali reactivity approach, 11th International Conference on Alkali-Aggregate Reaction in Concrete, Bérubé M.A. Fournier B. Durand B. (Editors), Quebec City, Canada, 2000, 335-344.
[9] Lombardi J. Perruchot A. Massard P. Larive C., « Etude comparée des gels silico-calciques produits des réactions alcalis-granulats dans les bétons et de gels synthétiques types », Cement and Concrete Research, Vol. 26, pp. 623-631, 1996.
[10] Jones A.E., Clark L.A., 1996, "The effects of restraint on ASR expansion of reinforced concrete", Magazine of Concrete Research, 48, N°174, pp. 1-13.
[11] Larive C., Laplaud A., Joly M., 1996, "Behavior of AAR-affected concrete: Experimental data", 10th International Conference on Alkali-Aggregate Reaction, Melbourne, Australia, pp. 670-677.
[12] Léger P., Cote P., Tinawi R., 1996, "Finite element analysis of concrete swelling due to Alkali-Aggregate Reaction in Dams", Computer and Structures, Vol. 60, pp. 601-611.
[13] Li, K., and Coussy, O., 2002, "Concrete ASR Degradation: From Material Modeling to Structure Assessment," Journal of Concrete Science and Engineering, V. 4, pp. 35-46.
[14] LPC. 1997 : LPC N°44 « Alcali réaction du béton : essai d'expansion résiduelle sur béton durci, à 38°C et H.R. ≥ 95% », presse des ponts et chaussées, Février 1997, in french.
[15] Moisson M., Cyr M., Ringot E., Carles-Gibergues A., Efficiency of reactive aggregate powder in controlling the expansion of concrete affected by alkali-silica reaction (ASR), 12th International Conference on Alkali-Aggregate Reaction in Concrete, Tang M. and Deng M. (Editors), Beijing, China, 2004, pp.617-624.
[16] Multon & al. 2008 : S. Multon, M. Cyr, A. Sellier, P. Diederich, L. Petit , "Effects of aggregate size and alkali content on ASR expansion", submitted to ICAAR13.
[17] Multon & al. 2008 : Multon S., Barin F-X., Godart B., Toutlemonde F., "Estimation of the Residual Expansion of Concrete Affected by AAR", Journal of Materials in Civil Engineering, ASCE 0899-1561, Vol. 20, No. 1, January 2008.
[18] Multon S., Toutlemonde F., 2006, "Effect of Applied Stresses on Alkali-Silica Reaction Induced Expansions", Cement and Concrete Research, Vol. 36, n°5, pp. 912-920.
[19] Poyet & al. 2007 : Poyet S., Sellier A., Capra B., Foray G., Torrenti J.-M., Cognon H. & Bourdarot E., "Chemical modelling of Alkali Silica reaction: Influence of the reactive aggregate size distribution", Materials & Structures , Vol. 40, pp. 229-239, 2007.
[20] Poyet & al. 2006 : Stéphane Poyet - Alain Sellier - Bruno Capra - Genevieve Thèvenin-Foray - Jean-Michel Torrenti - Hélène Tournier-Cognon - Eric Bourdarot, "Influence of water on Alkali-Silica Reaction: Experimental study and numerical simulations", Journal of Material in Civil Engineering, 10.1061©ASCE 0899-1561, Vol. 18 No 4 August 2006.
[21] Malla S., Wieland M., 1999, 'Analysis of an arch-gravity dam with a horizontal crack', Computers and Structures 72 (1999) 267-278.
[22] Sellier A., Bary B. "Coupled damage tensors and weakest link theory for describing crack induced orthotropy in concrete", Engineering Fracture Mechanics n°1629, may 2002.
[23] Ulm F.-J., Coussy O., Li K., Larive C., 2000, "Thermo-Chemo-Mechanics of ASR expansion in concrete structures", J. Eng. Mech, Vol. 126, n°3, pp. 233-242.
[24] Victor Saouma, Luigi Perotti, and Takashi Shimpo, 2007, 'Stress Analysis of Concrete Structures Subjected to Alkali-Aggregate Reactions', ACI Material Journal, 104(5), 532-541.

TABLE 1: gel volume kinetic constants and kinetic constants for each aggregate size class.

Concrete Type	Size range	Mortar type	f	A_T	α_0	τ (year)
C250	5-100	G250	2.%	0.12	0.0026	522
	0-5	S250		0.49	0.012	84
C350	5-30	G350		0.42	0.010	101
	0-5	S250		0.61	0.017	58

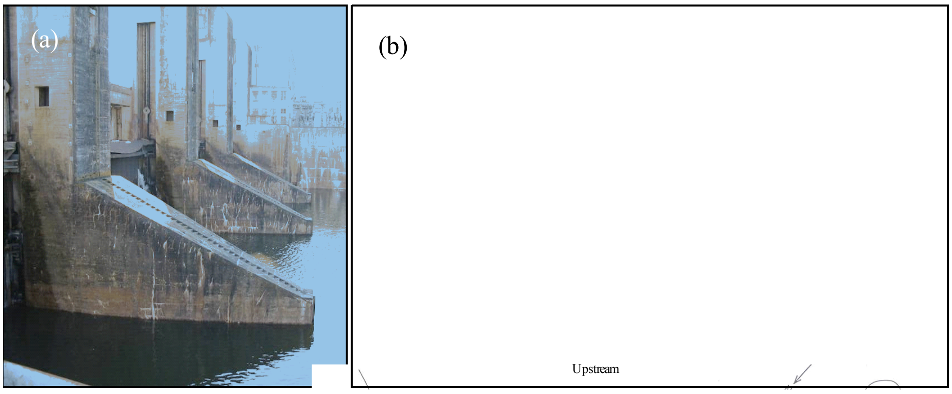

Figure 1 : Overview (a) and Upper view scheme (b) of the dam.

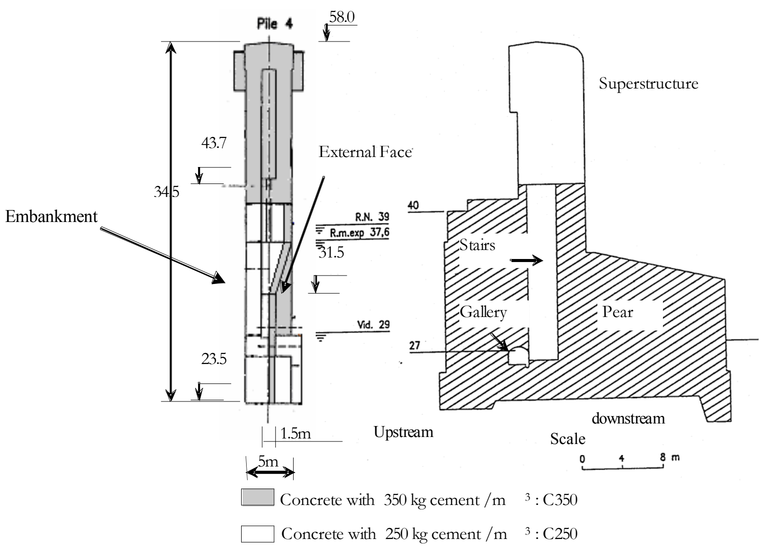

Figure 2 : Downstream and transversal views of the dam's pile studied, and definition of concrete types.

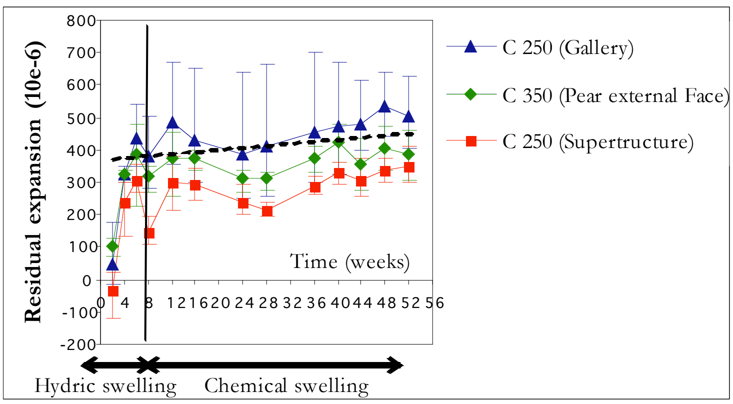

Figure 3 : Longitudinal strain of core samples under classical residual swelling tests (line: experiment, dotted line: tendency).

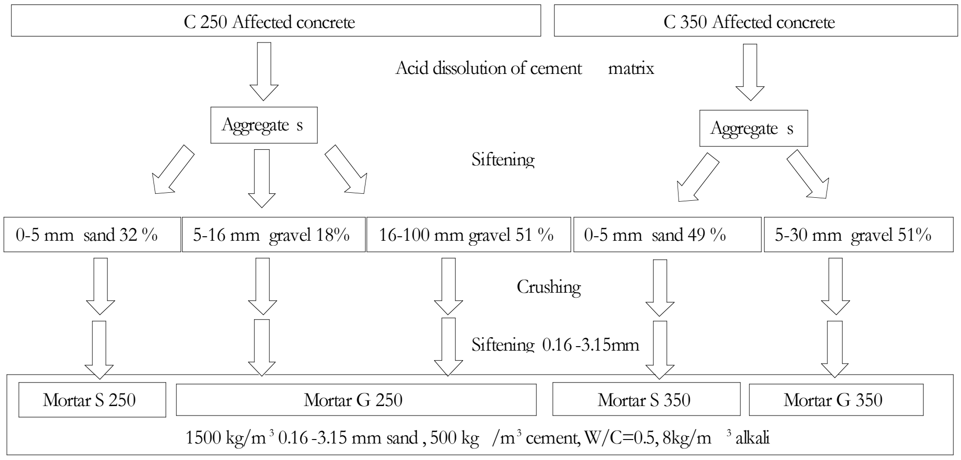

Figure 4 : Mortar confection procedure using aggregates recovered from C 250 and C 350 affected concretes.

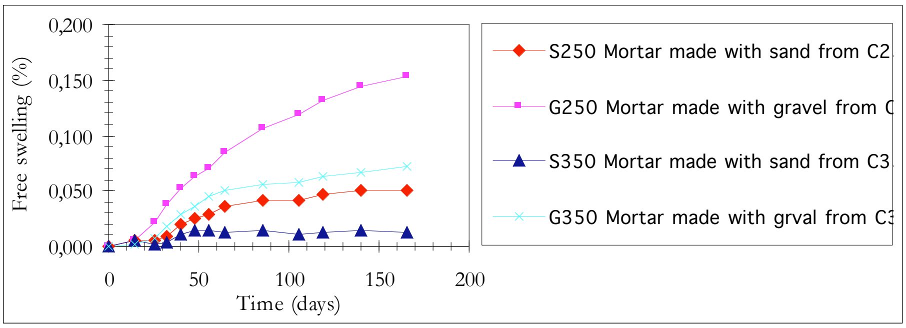

Figure 5: Mortar specimens swelling (dots), fitted curves (dotted lines).

Figure 6 : Peripheral altered zone by AAR in a large concrete aggregate.

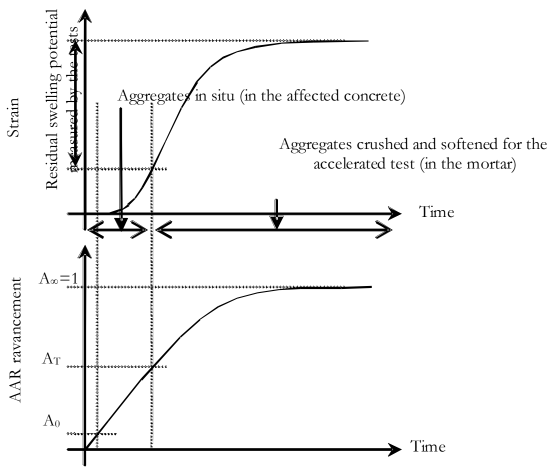

Figure 7 : Principle of chemical advancement assessment.

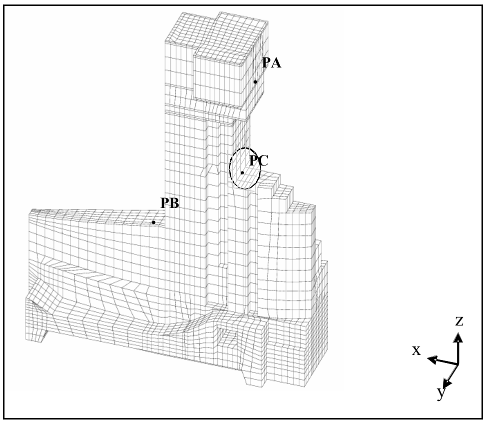

Figure 8 : Mesh of the pile 4; Points chosen for in situ displacement measures.

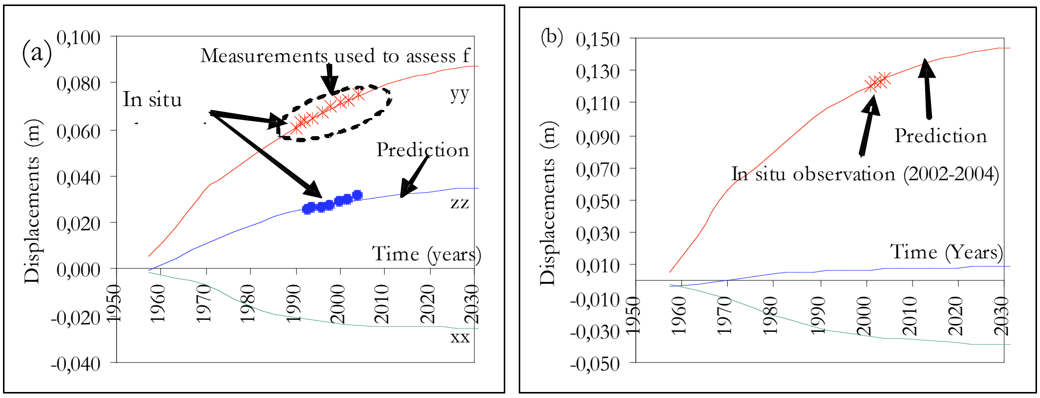

Figure 9 : (a) Fitting of the swelling amplitude on the structural displacements (point PC direction yy), prediction for Pc direction zz and xx, extrapolation for the next decades, (b) PA displacements, confrontation to in situ observations and prediction for the next decades.

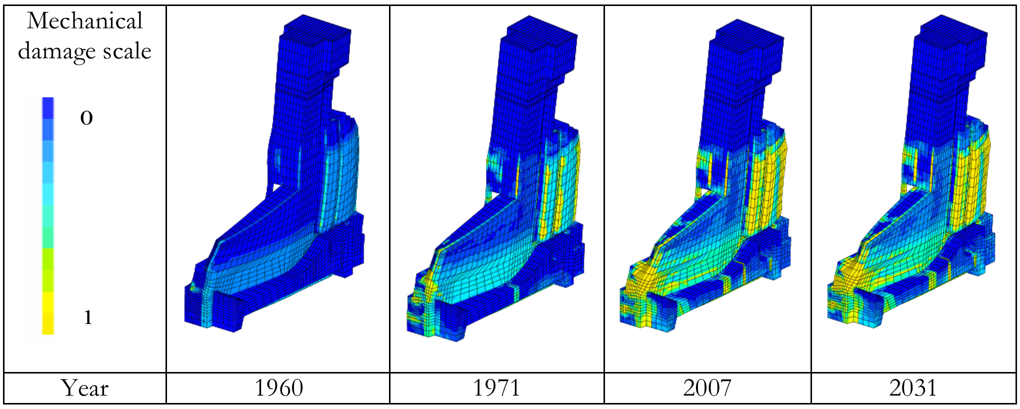

Figure 10 : Tensile damage evolution on deformed mesh (Damage equal to zero: no crack, damage equal to one: macroscopic cracks).